Supplementary File

Rui Tan, *Member, IEEE*, Guoliang Xing, *Member, IEEE*, Benyuan Liu, *Member, IEEE*, Jianping Wang, *Member, IEEE*, and Xiaohua Jia, *Senior Member, IEEE*

This document includes the supplemental materials for the paper titled "Exploiting Data Fusion to Improve the Coverage of Wireless Sensor Networks."

APPENDIX

A. Summary of Notation

Table II summarizes the notation used in the paper.

TABLE II
SUMMARY OF NOTATION*

Symbol	Definition
S	original signal energy emitted by the target
μ, σ^2	mean and variance of noise energy
δ	peak signal-to-noise ratio (PSNR), $\delta = S/\sigma$
k	path loss exponent
$w(\cdot)$	signal decay function, $w(x) = \Theta(x^{-k})$
d_i	distance from the target
s_i	attenuated signal energy, $s_i = S \cdot w(d_i)$
n_i	noise energy, $n_i \sim \mathcal{N}(\mu, \sigma^2)$
y_i	signal energy measurement, $y_i = s_i + n_i$
P_F / P_D	false alarm rate / detection probability
α / β	upper / lower bound of P_F / P_D
H_0 / H_1	hypothesis that the target is absent / present
ρ	network density
l	grid side length of regular network
$\mathbf{F}(p)$	the set of sensors within fusion range of point p
$N(p)$	the number of sensors in $\mathbf{F}(p)$
ϵ	upper bound of target localization error

* The symbols with subscript i refer to the notation of sensor i.

B. Optimal Value Fusion Rule

Suppose there are N sensors taking part in the data fusion. The optimal decision rule that minimizes the average cost (*i.e.*, Bayesian decision) is given by the likelihood ratio test:

$$\frac{p(y_1, \ldots, y_N|H_1)}{p(y_1, \ldots, y_N|H_0)} \underset{H_0}{\overset{H_1}{\gtrless}} \frac{P_0(C_{10} - C_{00})}{P_1(C_{01} - C_{11})}.$$

where $P_0 = \mathbb{P}(H_0)$, $P_1 = \mathbb{P}(H_1)$, and C_{ij} is the cost that we decide H_i when the ground truth is H_j. The left-hand side is the likelihood ratio and the right-hand side is the optimal Bayes threshold. As the sensors' measurements are independent Gaussians assumed in Section III-A, we have

$$\frac{p(y_1, \ldots, y_N|H_1)}{p(y_1, \ldots, y_N|H_0)} = \prod_{i=1}^{N} \frac{p(y_i|H_1)}{p(y_i|H_0)} = \mathrm{e}^{\sum_{i=1}^{N} \frac{2s_i y_i - 2\mu s_i - s_i^2}{\sigma^2}}.$$

Accordingly, the likelihood ratio test becomes

$$\sum_{i=1}^{N} \frac{s_i}{\sigma} \cdot y_i \underset{H_0}{\overset{H_1}{\gtrless}} \frac{1}{2} \sum_{i=1}^{N} \frac{2\mu s_i + s_i^2}{\sigma} + \frac{\sigma}{2} \ln \frac{P_0(C_{10} - C_{00})}{P_1(C_{01} - C_{11})}.$$

Therefore, the optimal fusion statistic for Bayesian decision is $\sum_{i=1}^{N} \frac{s_i}{\sigma} \cdot y_i$ where $\frac{s_i}{\sigma}$ is the received signal-to-noise ratio (SNR) of sensor i.

C. Proofs

C.1. Proof of Lemma 1

Proof: We first discuss the necessary and sufficient condition that p is (α, β)-covered. When no target is present, all sensors measure independent and identically distributed (*i.i.d.*) noises and hence $Y|H_0 = \sum_{i \in \mathbf{F}(p)} n_i \sim \mathcal{N}(\mu N(p), \sigma^2 N(p))$. Therefore, the false alarm rate is $P_F = \mathbb{P}(Y \geq T|H_0) = Q\left(\frac{T - \mu N(p)}{\sigma\sqrt{N(p)}}\right)$, where T is the detection threshold. As P_D is a non-decreasing function of P_F [1], it is maximized when P_F is set to be the upper bound α. Such a scheme is referred to as the Constant False Alarm Rate detector [1]. Let $P_F = \alpha$, the optimal detection threshold can be derived as $T_{\text{opt}} = \mu N(p) + \sigma Q^{-1}(\alpha)\sqrt{N(p)}$.

When the target is present, $Y|H_1 = \sum_{i \in \mathbf{F}(p)} s_i + n_i \sim \mathcal{N}(\mu N(p) + \sum_{i \in \mathbf{F}(p)} s_i, \sigma^2 N(p))$. Therefore, the detection probability at p is given by $P_D(p) = \mathbb{P}(Y \geq T|H_1) = Q\left(\frac{T - \mu N(p) - \sum_{i \in \mathbf{F}(p)} s_i}{\sigma\sqrt{N(p)}}\right)$. By replacing T with T_{opt} and solving $P_D(p) \geq \beta$, we have the necessary and sufficient condition that p is (α, β)-covered:

$$\frac{\sum_{i \in \mathbf{F}(p)} s_i}{\sqrt{N(p)}} \geq \sigma \left(Q^{-1}(\alpha) - Q^{-1}(\beta)\right). \tag{13}$$

As the random network is stationary, the fraction of covered area equals the probability that an arbitrary point is covered by the network [2]. Therefore, the (α, β)-coverage of the network is given by (5). ■

C.2. Proof of Lemma 2

Proof: We first prove that the $\{s_i | i \in \mathbf{F}(p)\}$ are *i.i.d.* for given p and derive the formulas for μ_s and σ_s^2. As sensors are deployed uniformly and independently, $\{d_i | i \in \mathbf{F}(p)\}$ are

This work was supported in part by the National Science Foundation under grants CNS-0954039 (CAREER) and ECCS-1029683.

Rui Tan and Guoliang Xing are with Department of Computer Science and Engineering, Michigan State University, USA. (e-mail: tanrui@gmail.com, glxing@msu.edu).

Jianping Wang and Xiaohua Jia are with Department of Computer Science, City University of Hong Kong, HKSAR. (e-mail: {jianwang, csjia}@cityu.edu.hk).

Benyuan Liu is with Department of Computer Science, University of Massachusetts Lowell, USA. (e-mail: bliu@cs.uml.edu).

i.i.d. for given p, where d_i is the distance between sensor i and point p. To simplify our discussion, we now temporarily assume that there is no localization error, *i.e.*, $\epsilon = 0$. Therefore, $\{s_i | i \in \mathbf{F}(p)\}$ are *i.i.d.* for given p, as s_i is a function of d_i (*i.e.*, $s_i = S \cdot w(d_i)$). Suppose the coordinates of point p and sensor i are (x_p, y_p) and (x_i, y_i), respectively. The posterior probability density function of (x_i, y_i) is $f(x_i, y_i) = \frac{1}{\pi R^2}$ where $(x_i - x_p)^2 + (y_i - y_p)^2 \leq R^2$. Hence, the posterior cumulative distribution function (CDF) of d_i is given by $F(d_i) = \int_0^{2\pi} \mathrm{d}\theta \int_0^{d_i} \frac{1}{\pi R^2} \cdot x \mathrm{d}x = \frac{d_i^2}{R^2}$ where $d_i \in [0, R]$. Therefore, we have

$$\mu_s = \int_0^R s_i \mathrm{d}F(d_i) = \frac{2S}{R^2} \cdot \int_0^R x w(x) \mathrm{d}x,$$
$$\sigma_s^2 = \int_0^R s_i^2 \mathrm{d}F(d_i) - \mu_s^2 = \frac{2S^2}{R^2} \int_0^R x w^2(x) \mathrm{d}x - \mu_s^2.$$

A straightforward approximation is to replace $\sum_{i \in \mathbf{F}(p)} s_i$ in (5) with its mean $\mu_s N(p)$. However, doing so ignores the distribution of $\sum_{i \in \mathbf{F}(p)} s_i$. We approximate $\sum_{i \in \mathbf{F}(p)} s_i$ as a Gaussian random variable according to the Central Limit Theorem (CLT), *i.e.*, $\sum_{i \in \mathbf{F}(p)} s_i \sim \mathcal{N}(\mu_s N(p), \sigma_s^2 N(p))$. Note that here we treat $N(p)$ as a constant. When the target is present, $Y|H_1 = \sum_{i \in \mathbf{F}(p)} s_i + \sum_{i \in \mathbf{F}(p)} n_i$. As the sum of two independent Gaussians is also Gaussian, $Y|H_1$ follows the normal distribution, *i.e.*, $Y|H_1 \sim \mathcal{N}(\mu_s N(p) + \mu N(p), \sigma_s^2 N(p) + \sigma^2 N(p))$. Therefore, the detection probability at point p is given by $P_D(p) = \mathbb{P}(Y \geq T|H_1) \simeq Q\left(\frac{T - \mu_s N(p) - \mu N(p)}{\sqrt{\sigma_s^2 + \sigma^2} \cdot \sqrt{N(p)}}\right)$. By replacing T with the optimal detection threshold T_{opt} (derived in the proof of Lemma 1) and solving $P_D(p) \geq \beta$, the condition that p is (α, β)-covered is given by $N(p) \geq \gamma(R)$. The approximate formula of (α, β)-coverage is then given by

$$c \simeq \mathbb{P}(N(p) \geq \gamma(R)) = 1 - F_{\text{Poi}}(\gamma(R) | \rho\pi R^2), \qquad (14)$$

where $F_{\text{Poi}}(\cdot|\lambda)$ is the CDF of the Poisson distribution $\text{Poi}(\lambda)$. When $\rho\pi R^2$ is large enough, the Poisson distribution $\text{Poi}(\rho\pi R^2)$ can be excellently approximated by the normal distribution $\mathcal{N}(\rho\pi R^2, \rho\pi R^2)$. Therefore, Eq. (14) can be further approximated by (6). ■

C.3. Proof of Lemma 3

Proof: For any point p, $\sum_{i \in \mathbf{F}(p)} s_i \geq S \cdot w(R + \epsilon) \cdot N(p)$, as $s_i \geq S \cdot w(R + \epsilon)$ for any sensor i in $\mathbf{F}(p)$. If $\frac{S \cdot w(R+\epsilon) \cdot N(p)}{\sqrt{N(p)}} \geq \sigma\left(Q^{-1}(\alpha) - Q^{-1}(\beta)\right)$, Eq. (13) must hold. Therefore, by solving $N(p)$, the sufficient condition that p is (α, β)-covered is $N(p) \geq \Gamma(R)$. Moreover, as $N(p) \sim \text{Poi}(\rho\pi R^2)$, we have

$$\begin{aligned} c &= \mathbb{P}(\text{point } p \text{ is } (\alpha, \beta)\text{-covered}) \\ &\geq \mathbb{P}(N(p) \geq \Gamma(R)) \\ &= 1 - F_{\text{Poi}}(\Gamma(R) | \rho\pi R^2). \end{aligned}$$

Therefore, the lower bound of c is given by (7). When $\rho\pi R^2$ is large enough, the normal distribution $\mathcal{N}(\rho\pi R^2, \rho\pi R^2)$ excellently approximates the Poisson distribution $\text{Poi}(\rho\pi R^2)$. Therefore, Eq. (7) can be approximated by (9). ■

C.4. Proof of Theorem 1

Proof: As ρ_f is large to provide a high level of coverage under the fusion model, the lower bound of (α, β)-coverage, c_L, is given by (9) according to Lemma 3. We define $h_1(\rho_f) = \frac{\Gamma(R)}{\sqrt{\pi} R} \cdot \frac{1}{\sqrt{\rho_f}}$, $h_2(\rho_f) = \sqrt{\pi} R \cdot \sqrt{\rho_f}$ and hence $c_L = Q(h_1(\rho_f) - h_2(\rho_f))$. When $\rho_f \to \infty$, $h_2(\rho_f)$ dominates $h_1(\rho_f)$ as $\lim_{\rho_f \to \infty} \frac{h_1(\rho_f)}{h_2(\rho_f)} = 0$. Hence, $c \geq c_L = Q(-h_2(\rho_f)) = Q(-\sqrt{\pi} R \cdot \sqrt{\rho_f})$ when $\rho_f \to \infty$. Define $x = Q^{-1}(c)$. We have $\rho_f \leq \frac{1}{\pi R^2} x^2$ when $c \to 1$.

Under the disc model, by replacing $c = Q(x) = 1 - \Phi(x)$ in (3) and solving ρ_d, we have $\rho_d = -\frac{1}{\pi r^2} \ln \Phi(x)$, where $\Phi(x)$ is the CDF of the standard normal distribution. Hence, we have

$$\lim_{c \to 1} \frac{\rho_f}{\rho_d} \leq \lim_{x \to -\infty} \frac{\frac{1}{\pi R^2} x^2}{-\frac{1}{\pi r^2} \ln \Phi(x)} = -\frac{r^2}{R^2} \lim_{x \to -\infty} \frac{x^2}{\ln \Phi(x)}.$$

As $\lim_{x \to -\infty} \frac{x^2}{\ln \Phi(x)} = -2$ (derived in Appendix C.10), we have $\lim_{c \to 1} \frac{\rho_f}{\rho_d} \leq \frac{2r^2}{R^2}$. Therefore, the asymptotic upper bound of ρ_f is given by (10). ■

C.5. Proof of Theorem 2

Proof: We choose R by

$$\frac{\xi}{\pi} \cdot \frac{\Gamma(R)}{R^2} = \rho_f, \qquad (15)$$

where ξ is a constant and $\xi > 1$. It is easy to verify that the chosen R is order-optimal for the lower bound of coverage (*i.e.*, c_L). Moreover, it is easy to verify that both the chosen R and $\Gamma(R)$ increase with ρ_f. By replacing ρ_f in (9) with (15), c_L is given by $c_L = Q\left(\left(\frac{1}{\sqrt{\xi}} - \sqrt{\xi}\right) \cdot \sqrt{\Gamma(R)}\right) = 1 - \Phi(\eta z)$, where $\eta = \frac{1}{\sqrt{\xi}} - \sqrt{\xi}$ is a constant and $z = \sqrt{\Gamma(R)}$. Hence we have $c \geq c_L = 1 - \Phi(\eta z)$. According to (3), the network density under the disc model satisfies $\rho_d = -\frac{1}{\pi r^2} \ln(1 - c) \geq -\frac{1}{\pi r^2} \ln \Phi(\eta z)$. Hence, the ratio ρ_f^b / ρ_d where b is a positive constant satisfies

$$\begin{aligned} \lim_{c \to 1} \frac{\rho_f^b}{\rho_d} &\leq \lim_{R \to \infty} \frac{\left(\frac{\xi}{\pi}\right)^b \cdot \frac{\Gamma^b(R)}{R^{2b}}}{-\frac{1}{\pi r^2} \ln \Phi(\eta z)} \\ &= -\frac{\xi^b r^2}{\pi^{b-1}} \cdot \lim_{z \to \infty} \frac{z^2}{\ln \Phi(\eta z)} \cdot \lim_{R \to \infty} \frac{\Gamma^{b-1}(R)}{R^{2b}} \\ &= \frac{2\xi^b r^2}{\pi^{b-1} \eta^2} \cdot \lim_{R \to \infty} \frac{\Gamma^{b-1}(R)}{R^{2b}}. \end{aligned}$$

Note that $\lim_{z \to \infty} \frac{z^2}{\ln \Phi(\eta z)} = -\frac{2}{\eta^2}$ (derived in Appendix C.10) in the above derivation. As $w(x) = \Theta(x^{-k})$ and ϵ is constant, $\Gamma(R) = \Theta(1/w^2(R + \epsilon)) = \Theta((R + \epsilon)^{2k}) = \Theta(R^{2k})$ and hence $\Gamma^{b-1}(R) = \Theta(R^{2kb-2k})$. Therefore, $\lim_{R \to \infty} \frac{\Gamma^{b-1}(R)}{R^{2b}} = \lim_{R \to \infty} R^{2kb-2k-2b}$. If $b \leq \frac{k}{k-1}$, $\lim_{R \to \infty} \frac{\Gamma^{b-1}(R)}{R^{2b}}$ is a constant and hence $\lim_{c \to 1} \frac{\rho_f^b}{\rho_d}$ is upper-bounded by a constant. Hence, we have (11). We note that although the chosen R is not optimal for c, the upper bound given by (11) still holds if R is optimal for c. ■

C.6. Proof of Corollary 1

Proof: As $w(x) = \Theta(x^{-k})$, $w^{-1}(x) = \Theta(x^{-1/k})$. According to (2), the sensing range $r = \Theta(\delta^{1/k})$. As $\lim_{c\to 1} \frac{\rho_f}{\rho_d} \leq \frac{2r^2}{R^2} = \Theta(\delta^{2/k})$, we have $\frac{\rho_f}{\rho_d} = \mathcal{O}(\delta^{2/k})$ when $c \to 1$. ■

C.7. Proof of Lemma 4

Proof: As proved in Lemma 3, the sufficient condition that an arbitrary point p is (α, β)-covered is $N(p) \geq \Gamma(R)$, where $\Gamma(R)$ is given by (8). Moreover, it has been proved in [3] that if the grid side length is chosen to be $l = \frac{\sqrt{2}R}{\sqrt{\Gamma(R)}}$, there will be at least $\Gamma(R)$ grid points within the disc of radius R centered at any point. Hence, the network density of $\frac{1}{l^2}$ is sufficient to guarantee full coverage of regular networks. Therefore, the minimum network density ρ_f for achieving full coverage is upper-bounded by $\frac{1}{l^2} = \frac{\Gamma(R)}{2R^2}$. By replacing $\Gamma(R)$ with (8), we have (12). ■

C.8. Proof of Theorem 3

Proof: The upper-bound of ρ_f is given by (12) and ρ_d is given by (4). If the localization error ϵ is insignificant such that $\epsilon \ll R$, we can consider $w^2(R+\epsilon) \simeq w^2(R)$ in (12). Hence, the ratio of network densities satisfies

$$\frac{\rho_f}{\rho_d} \leq \frac{\left(Q^{-1}(\alpha) - Q^{-1}(\beta)\right)^2 \cdot r^2}{\delta^2 \cdot R^2 \cdot w^2(R)}.$$

By letting $R = r = w^{-1}\left(\frac{Q^{-1}(\alpha)-Q^{-1}(\beta)}{\delta}\right)$, we have $\frac{\rho_f}{\rho_d} \leq 1$. ■

C.9. Proof of Corollary 2

Proof: For fixed fusion range R, the grid side length l must satisfy $l \leq \sqrt{2}R$ to ensure at least one sensor within the fusion range. When the SNR is sufficiently high, only one sensor within the fusion range is enough to meet the performance requirements α and β. Therefore, we can choose the grid side length $l = \sqrt{2}R$ and the minimum network density is given by $\rho_f = \frac{1}{l^2} = \frac{1}{2R^2}$. Hence, $\frac{\rho_f}{\rho_d} = \frac{r^2}{R^2} = \mathcal{O}(r^2)$. Moreover, as $r = \Theta\left(\delta^{1/k}\right)$ (proved in Corollary 1), we have $\frac{\rho_f}{\rho_d} = \mathcal{O}\left(\delta^{2/k}\right)$. ■

C.10. Two Limits Used in the Proofs of Theorems 1 and 2

Denote $\phi(x)$ as the probability density function of the standard normal distribution, *i.e.*, $\phi(x) = \frac{1}{\sqrt{2\pi}}\mathrm{e}^{-x^2/2}$. Note that $\Phi'(x) = \phi(x)$ and $\phi'(x) = -x\phi(x)$. For constant $\eta < 0$, we have

$$\begin{aligned}
\lim_{z\to\infty} \frac{z^2}{\ln \Phi(\eta z)} &\overset{(*)}{=} \lim_{z\to\infty} \frac{2z}{\frac{1}{\Phi(\eta z)}\phi(\eta z)\eta} = \frac{2}{\eta} \lim_{z\to\infty} \frac{\Phi(\eta z) z}{\phi(\eta z)} \\
&\overset{(*)}{=} \frac{2}{\eta} \lim_{z\to\infty} \frac{\phi(\eta z)\eta z + \Phi(\eta z)}{-\eta^2 z \phi(\eta z)} = -\frac{2}{\eta^3}\left(\eta + \lim_{z\to\infty} \frac{\Phi(\eta z)}{z\phi(\eta z)}\right) \\
&\overset{(*)}{=} -\frac{2}{\eta^3}\left(\eta + \lim_{z\to\infty} \frac{\phi(\eta z)\eta}{\phi(\eta z) - \eta^2 z^2 \phi(\eta z)}\right) \\
&= -\frac{2}{\eta^3}\left(\eta + \lim_{z\to\infty} \frac{\eta}{1-\eta^2 z^2}\right) = -\frac{2}{\eta^2},
\end{aligned}$$

where the steps marked by (*) follow from the l'Hôpital's rule. Note that for $\eta < 0$, $\lim_{z\to\infty} \Phi(\eta z) z = 0$ and $\lim_{z\to\infty} z\phi(\eta z) = 0$. By replacing $z = -x$ and $\eta = -1$, we have

$$\lim_{x\to-\infty} \frac{x^2}{\ln \Phi(x)} = -2.$$

D. Extended Mobile Relocation Strategies

This appendix provides the illustration of the two extended mobile relocation strategies discussed in Section VII-B. The illustration is in Fig. 8.

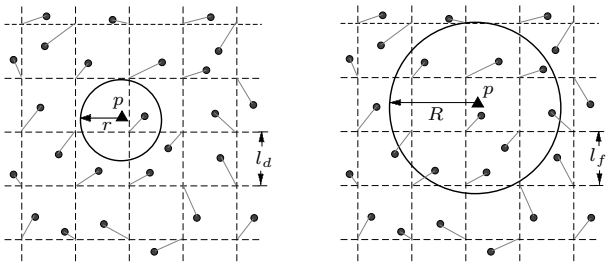

(a) (b)

Fig. 8. Extended mobile relocation strategies, where solid dots represent mobile sensors. (a) Under the probabilistic disc model, for any point p, there is at least one sensor within the circle of radius r given by (2), where the grid side length $l_d = \sqrt{2}r$; (b) Under the data fusion model, for any point p, there are at least $\Gamma(R)$ sensors within the fusion range of p, where the grid side length $l_f = \frac{\sqrt{2}R}{\sqrt{\Gamma(R)}}$.

E. Discussions

In this section, we discuss how to extend several theoretical results derived in this paper to address other noise models, signal decay laws and fusion models. We then discuss the detection latency of data fusion.

1) Noise Models: In the proofs of Lemma 1, Lemma 2 and Lemma 3, the fusion statistic Y has a component $\sum_{i\in\mathbf{F}(p)} n_i$. According to the CLT, this component approximately follows the normal distribution if $\{n_i\}$ are *i.i.d.*. Therefore, the assumption of *i.i.d.* Gaussian noises made in Section III-A can be relaxed to *i.i.d.* noises that follow any distribution, when the number of sensors taking part in data fusion is large enough. In practice, the accuracy of this approximation is satisfactory when $N(p) \geq 20$ [4]. In particular, the distribution of noise will not affect the asymptotic scaling laws in Section VI, as $N(p)$ is large in the asymptotic scenarios where $c \to 1$.

2) Signal decay laws: The main objective of this paper is to explore the fundamental limits of coverage based on data fusion model in target surveillance applications, in which sensors measure the signals emitted by the target. The proofs of Lemma 1-4, Theorem 1 and 3 are not dependent on the form of the signal decay function $w(\cdot)$. Therefore, these results hold under *arbitrary* bounded decreasing function $w(\cdot)$. However, Theorem 2, Corollary 1 and 2 are only applicable for the applications where the target signal follows the power law decay, *i.e.*, $w(x) = \Theta(x^{-k})$. We acknowledge that most mechanical and electromagnetic waves follow the power law decay in propagation. In particular, in open space, inverse-square law (*i.e.*, $k = 2$) [5] applies to various physical signals such as sound, light and radiation. In our future work, we will extend our analyses to address other decay laws such as exponential decay in diffusion processes [6].

3) Data fusion models: Theorem 1-3 and Corollary 1-2 give the upper bounds of network density under the fusion model presented in Section III-B. If more efficient fusion models are employed, the coverage performance will be further improved. Therefore, more efficient fusion model can reduce the network density for achieving a certain level of coverage. As a result, the upper bounds of network density derived in this paper still hold. Exploring the impact of efficiency of fusion models on network density is left for future work.

We now briefly discuss how to extend our analysis framework to address decision fusion [7]. This discussion provides insights into the impact of sensor quantization on the asymptotic results presented in previous sections. In the decision fusion model, each sensor i makes a local decision I_i by camparing its measurement y_i against a *local threshold* λ. If $y_i \geq \lambda$, $I_i = 1$; otherwise, $I_i = 0$. Let Y denote the number of positive local decisions, *i.e.*, $Y = \sum_{i \in \mathbf{F}(p)} I_i$. The cluster head makes a system detection decision by a threshold testing, *i.e.*, given a *system threshold* $\theta \in [0, 1)$, if $\frac{Y}{N(p)} > \theta$, the cluster head decides H_1; otherwise, it decides H_0. Such a decision fusion model has been widely employed in previous analytical studies [1], [7]–[9] and real systems [10]. We have derived the approximate system detection performance of this decision fusion model in [11]. Specifically, the system false alarm rate is $P_F \simeq Q\left(\frac{(\theta-\alpha_0)\cdot N(p)}{\sqrt{(\alpha_0-\alpha_0^2)\cdot N(p)}}\right)$, where α_0 is the local false alarm rate of a sensor given by $\alpha_0 = Q\left(\frac{\lambda-\mu}{\sigma}\right)$. We can solve the local threshold λ from $P_F = \alpha$. Moreover, as shown in [11], the system detection probability can be calculated by $P_D = Q\left(\frac{\theta\cdot N(p)-\sum_{i\in\mathbf{F}(p)} P_D^i}{\sqrt{\sum_{i\in\mathbf{F}(p)}\left(P_D^i-(P_D^i)^2\right)}}\right)$, where P_D^i is the local detection probability of sensor i that is given by $P_D^i = Q\left(\frac{\lambda-\mu-s_i}{\sigma}\right)$. It has been shown in [11] that the P_D increases with $\sum_{i\in\mathbf{F}(p)} P_D^i$ with high probability. Therefore, $P_D \geq Q\left(\gamma\sqrt{N(p)}\right)$, where $\gamma = \frac{\theta-P_D^{\min}}{\sqrt{P_D^{\min}-(P_D^{\min})^2}}$ and $P_D^{\min}$ is the lower bound of P_D^i given by $P_D^{\min} = Q\left(\frac{\lambda-\mu-S\cdot w(R)}{\sigma}\right)$. As a result, the lower bound of coverage can be derived as $c_L = \mathbb{P}\left(Q\left(\gamma\sqrt{N(p)}\right) \geq \beta\right) = \mathbb{P}\left(N(p) \geq \Gamma(R)\right) = 1 - F_{\mathrm{Poi}}(\Gamma(R)|\rho\pi R^2)$, where $\Gamma(R) = \frac{\left(Q^{-1}(\beta)\right)^2}{\gamma^2}$. This result is consistent with Lemma 3. Accordingly, it is easy to verify that the asymptotic results for fixed R, *i.e.*, Theorem 1 and Corollary 1 are applicable to the decision fusion model. However, the proofs of other theorems and corollaries highly depend on the formula of $\Gamma(R)$. As the $\Gamma(R)$ for the decision fusion model is very complex, the extensions of other results to decision fusion model are still open issues.

In the above decision fusion model, the sensor reading is quantized into one bit. In the general quantization scheme [7], the sensor reading can be quantized into multiple bits. Intuitively, the sensing performance of the decision and value fusion models adopted in this paper lower-bounds and upper-bounds that of the general quantization scheme, respectively. In our future work, we plan to extensively investigate the trade-off between communication overhead and coverage performance of fusion-based wireless sensor networks (WSNs) with quantization.

4) Detection Latency of Data Fusion: We leverage the results presented in [12] to analyze the detection latency and guide the design of the data aggregation algorithm to minimize the latency. If the fusion range R is small such that each sensor in $\mathbf{F}(p)$ can directly communicate with each other, the best strategy is that the sensors communicate with the cluster head sequentially, leading to an average detection latency of $\Theta(\rho R^2)$. If the fusion range R is large such that a multi-hop cluster is needed to aggregate the sensor readings, the average detection latency is $\Theta(\log(\rho R^2))$. As shown in [12], to achieve this bound, the communication range of each sensor should be $\sqrt{\frac{2\log\rho}{\rho}}$. Moreover, the routing tree rooted at the cluster head is formed by grouping sensors according to a tessellation of the deployment region into square cells. More details of the optimal routing algorithm can be found in [12].

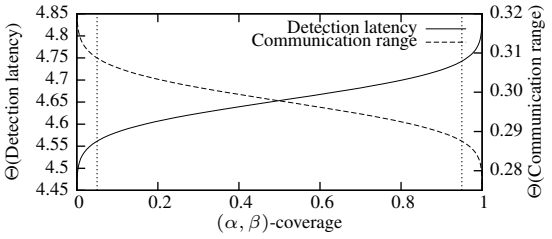

Fig. 9. Trade-off between detection latency and coverage ($\delta = 5000$, $R = 100$ m).

Fig. 9 plots the numerical result showing the trade-off between detection latency and (α, β)-coverage under the value fusion model. The tight bound of the optimal communication range is also plotted in the figure. We can see from the figure that a higher level of coverage is always achieved at the price of longer detection latency. Moreover, the detection latency and the coverage have an approximate linear relationship when the coverage is within $[0.05, 0.95]$. Note that if random media access control protocol (*e.g.*, CSMA/CA) is used, the detection latency will be larger than the above bounds because of the communication contention and backoffs. The further study on the fusion-based coverage problem that incorporates communication constraints such as connectivity and limited energy budget is left for our future work.

REFERENCES

[1] P. Varshney, *Distributed Detection and Data Fusion*. Springer, 1996.

[2] B. Liu and D. Towsley, "A study on the coverage of large-scale sensor networks," in *Proc. IEEE MASS*, 2004, pp. 475–483.

[3] W. Wang, V. Srinivasan, and K. C. Chua, "Trade-offs between mobility and density for coverage in wireless sensor networks," in *Proc. ACM MobiCom*, 2007, pp. 39–50.

[4] (2011) Nist/sematech e-handbook of statistical methods. [Online]. Available: http://itl.nist.gov/div898/handbook/

[5] D. Davis and C. Davis, *Sound System Engineering*. Focal Press, 1997.

[6] D. Stroock and S. Varadhan, *Multidimensional Diffusion Processes*. Springer, 1979.

[7] J. N. Tsitsiklis, "Decentralized detection," *Advances in Statistical Signal Processing*, vol. 2, 1993.

[8] T. Clouqueur, K. K. Saluja, and P. Ramanathan, "Fault tolerance in collaborative sensor networks for target detection," *IEEE Trans. Comput.*, vol. 53, no. 3, pp. 320–333, 2004.

[9] R. Niu and P. K. Varshney, "Distributed detection and fusion in a large wireless sensor network of random size," *EURASIP J. Wireless Communications and Networking*, vol. 2005, no. 4, pp. 462–472, 2005.

[10] T. He, S. Krishnamurthy, J. A. Stankovic, T. Abdelzaher, L. Luo, R. Stoleru, T. Yan, L. Gu, J. Hui, and B. Krogh, "Energy-efficient surveillance system using wireless sensor networks," in *Proc. MobiSys*, 2004, pp. 270–283.

[11] R. Tan, G. Xing, J. Wang, and H. C. So, "Exploiting reactive mobility for collaborative target detection in wireless sensor networks," *IEEE Trans. Mobile Comput.*, vol. 9, no. 3, pp. 317–332, 2010.

[12] A. Giridhar and P. R. Kumar, "Computing and communicating functions over sensor networks," *IEEE J-SAC*, vol. 23, no. 4, pp. 755–764, 2005.